Electronic Supplementary Material (ESI) for Journal of Materials Chemistry C.

Supporting Information

Efficient Solution-Processed Red All-Fluorescent Organic Light-Emitting Diodes Employing Thermally Activated Delayed Fluorescence Materials as Assistant Hosts: Molecular Design Strategy and Exciton Dynamic Analysis

Dongjun Chen,† Xinyi Cai,† Xianglong Li, Zuozheng He, Chengsong Cai, Dongcheng Chen and Shi-Jian Su*

State Key Laboratory of Luminescent Materials and Devices and Institute of Polymer Optoelectronic Materials and Devices, South China University of Technology, Guangzhou 510640, China

†These two authors contributed equally to this work.

*Corresponding author. E-mail: mssjsu@scut.edu.cn

1. Material information of DC-TC and DC-ACR.

Table S1. Thermal, electrochemical and photo-physical properties of DC-TC and DC-ACR[1]

Compound	T_d/T_g (˚C)[a,b]	λ_{abs} (nm)[c]	λ_{PL} (nm)[c]	PLQY (%)[c]	IP/EA (eV)[d]	$S_1/T_1/\Delta E_{ST}$ (eV)[e]
DC-TC	413/85	389	518	22.1	-5.58/-2.99	2.75/2.61/0.14
DC-ACR	387/98	411	532	8.0	-5.32/-2.79	2.48/2.47/0.01

[a] decomposition temperature (5% weight loss); [b] glass transition temperature; [c] PLQY of 15 wt% investigated molecules doped into CBP in N_2 atmosphere; [d] IP measured by cyclic voltammetry and EA calculated by IP minus optical gap approximated by absorption edge in toluene; [e] The values of the S_1, T_1 and ΔE_{ST} evaluated in toluene (DC-ACR in n-hexane) at 77K, respectively.

2. Surface morphology of the co-doped films.

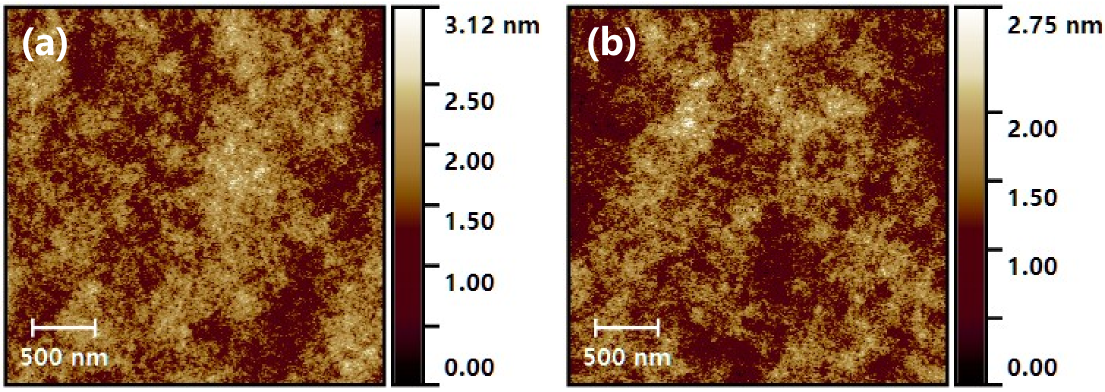

Figure S1. AFM images of 40-nm thin films of 2 wt% DBP:15 wt% DC-TC:CBP (a) and 2 wt% DBP:15 wt% DC-ACR:CBP (b) spin-coated on PEDOT:PSS coated ITO substrates. The films were prepared using chlorobenzene as the solvent and was then annealed at 100 °C for 10 min. The RMS roughness of 2 wt% DBP:15 wt% DC-TC:CBP and 2 wt% DBP:15 wt% DC-ACR:CBP films was 0.292 nm and 0.327 nm, respectively.

3. The PL characteristics and rate constants of TADF molecules.

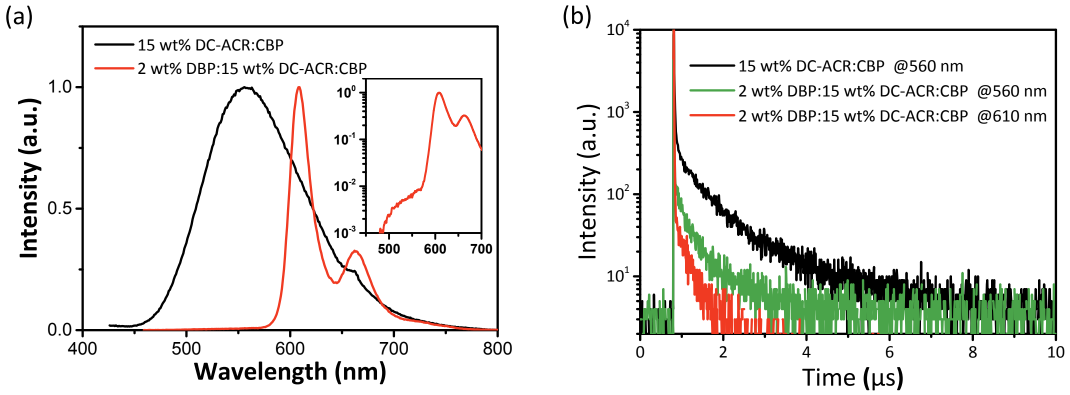

Figure S2. (a) The PL spectral of the co-doped films of 15 wt% DC-ACR:CBP (black line) and 2 wt% DBP:15 wt% DC-ACR:CBP (red line) in the air at room temperature. Inset shows the PL spectrum in logarithm. (b) Time-resolved fluorescence decay curves for the co-doped films of 15 wt% DC-ACR:CBP and 2 wt% DBP:15 wt% DC-ACR:CBP in a N_2 atmosphere.

Table S2. The PL efficiencies and life-times of the PL decay curves of the co-doped films.

Films	Φ (%)	Φ_F (%)	Φ_{TADF} (%)	τ_p (ns)	τ_d (μs)
15%DC-TC:CBP	22.1	12.3	9.7	16.72	14.29
2% DBP:15% DC-TC:CBP	69.2	55.1	14.1	5.37	1.34
15% DC-ACR:CBP	8.0	6.6	6.6	10.85	0.78
2% DBP:15% DC-ACR:CBP	62.1	48.7	13.4	5.56	0.37

With the measured PL efficiencies and decay times, the rate constants for the 15 wt% DC-TC:CBP and 15 wt% DC-ACR:CBP co-doped films were calculated using the equations described as follow:[2-6]

$$k_p = \frac{1}{\tau_p} \quad (1)$$

$$k_d = \frac{1}{\tau_d} \quad (2)$$

$$k_r^S = \Phi_F k_p \quad (3)$$

$$k_{nr}^S = \left(\frac{\Phi_F}{\Phi} - \Phi_F\right) k_p \quad (4)$$

$$k_{nr}^T = k_d - \Phi_F k_{RISC} \quad (5)$$

$$k_{ISC} = \left(1 - \frac{\Phi_F}{\Phi}\right) k_p \quad (6)$$

$$k_{RISC} = \frac{k_p k_d \Phi_{TADF}}{k_{ISC} \quad \Phi_F} \quad (7)$$

where τ_p is the transient decay time of the prompt component, τ_d is the transient decay time of the delayed component, and Φ_F and Φ_{TADF} are the prompt and delayed components of the PL quantum efficiency, respectively.

For the DC-TC:CBP film, $k_{p,D}$ can be described as

$$k_{p,D} = k_r^S + k_{ISC} + k_{nr}^S \quad (8)$$

For the DBP:DC-TC:CBP co-doped films, $k_{p,DA}$ can be described as

$$k_{p,DA} = k_r^S + k_{ISC} + k_{nr}^S + k_{ET} \qquad (9)$$

where k_{ET} is the rate constant of the Förster resonance energy transfer.

Thus, k_{ET} can be describe as[7]

$$k_{ET} = k_{p,DA} - k_{p,D} = {}^{1}/_{\tau_{DA}} - {}^{1}/_{\tau_{D}} \qquad (10)$$

where τ_{DA} is the prompt fluorescent lifetime of the film with DBP and τ_D is the prompt fluorescent lifetime of the film without DBP.

4. Device Fabrication and Measurements

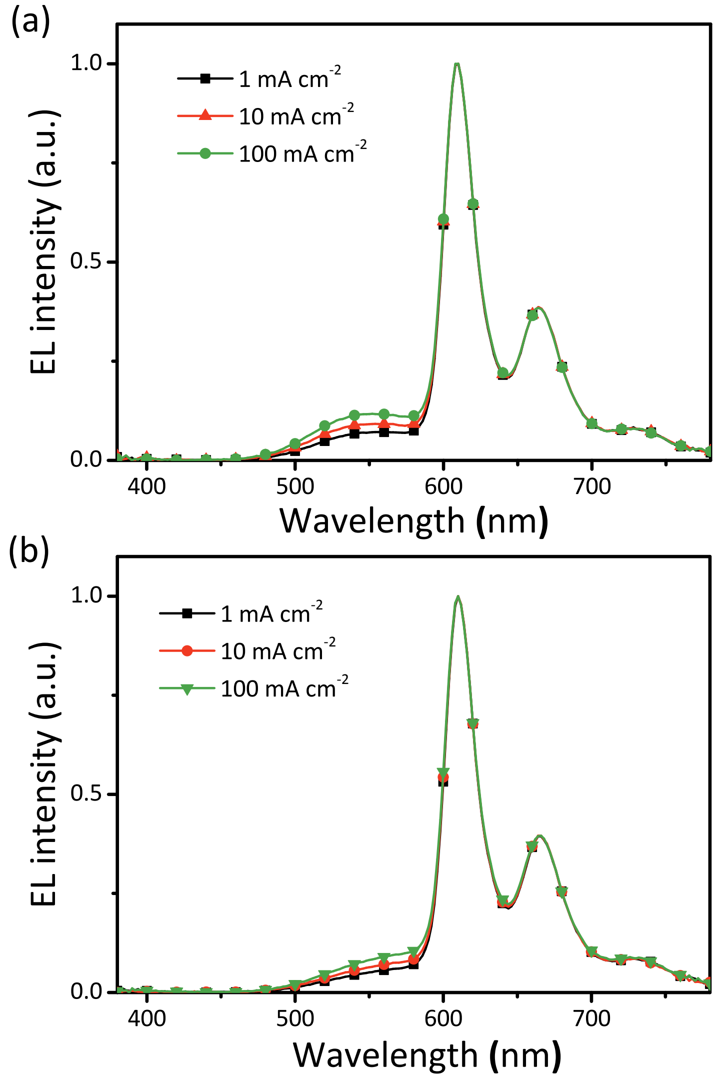

Figure S3. Normalized EL spectra of the devices using 2 wt% DBP:15 wt% DC-TC:CBP (a) or 2 wt% DBP:15 wt% DC-ACR:CBP (b) as EML under the current density ranging from 1 mA/m^2 to 100 mA/m^2.

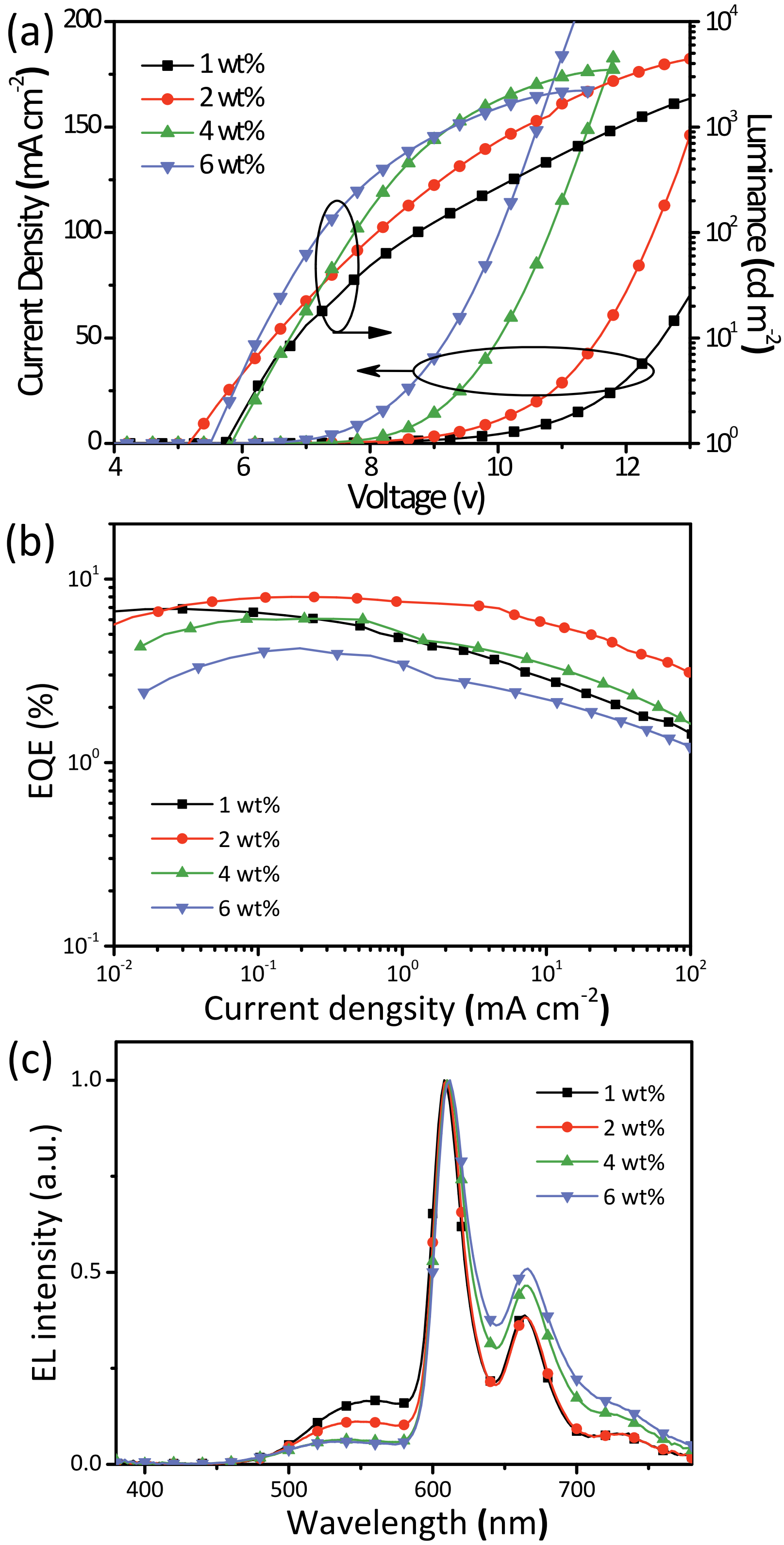

Figure S4. (a) Luminance-current density-voltage, (b) EQE-current density and (c) normalized EL spectra of the TAF-OLEDs based on DBP as an emitter at various doping concentrations in a structure of ITO/PEDOT:PSS (40 nm)/x wt% DBP:15 wt% DC-TC:CBP (40 nm)/TmPyPB (55 nm)/LiF (1 nm)/Al (100 nm).

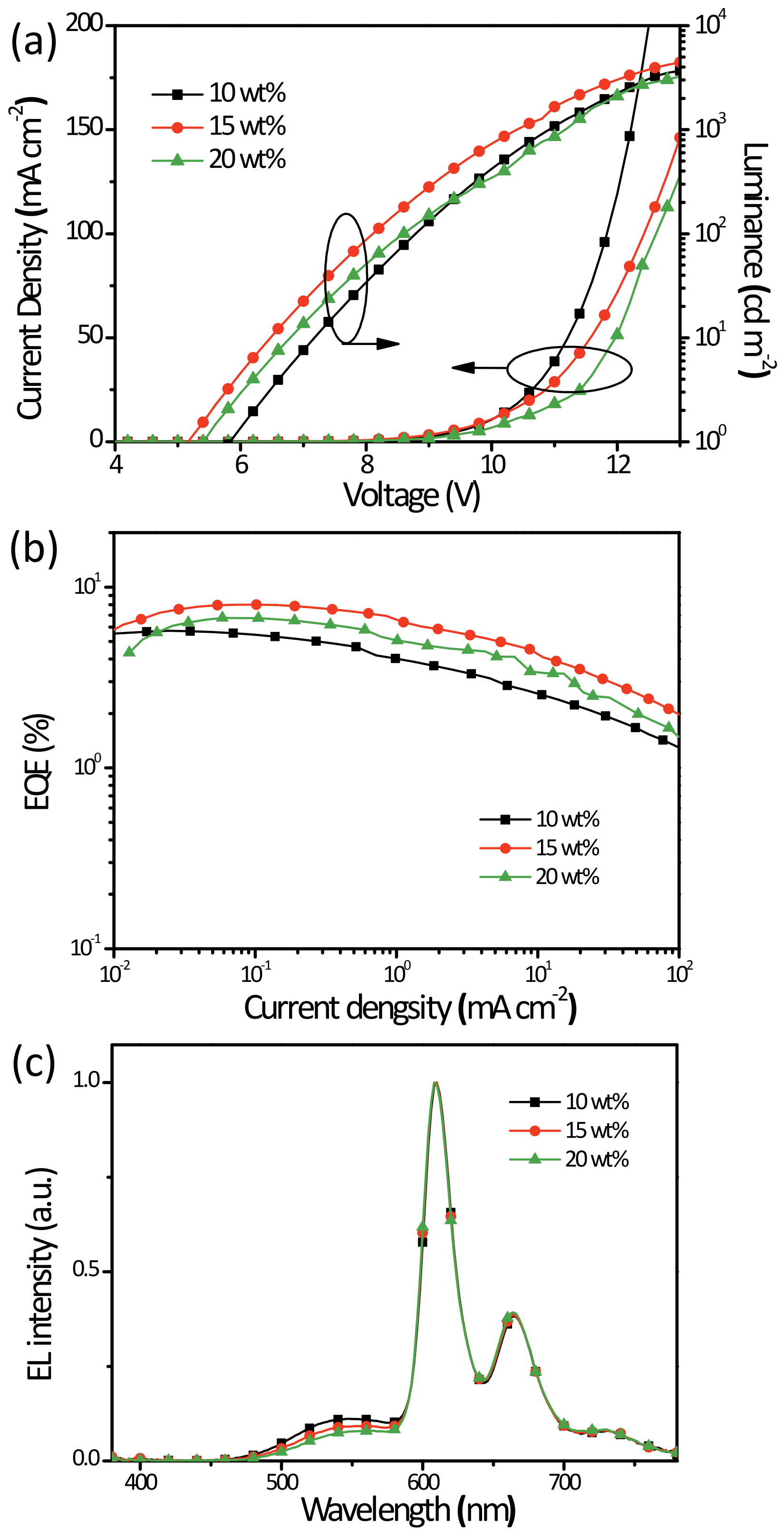

Figure S5. (a) Luminance-current density-voltage, (b) EQE-current density and (c) normalized EL spectra of the TAF-OLEDs based on DC-TC as an assistant dopant at various doping concentrations in a structure of ITO/PEDOT:PSS (40 nm)/2 wt% DBP:x wt% DC-TC:CBP (40 nm)/TmPyPB (55 nm)/LiF (1 nm)/Al (100 nm).

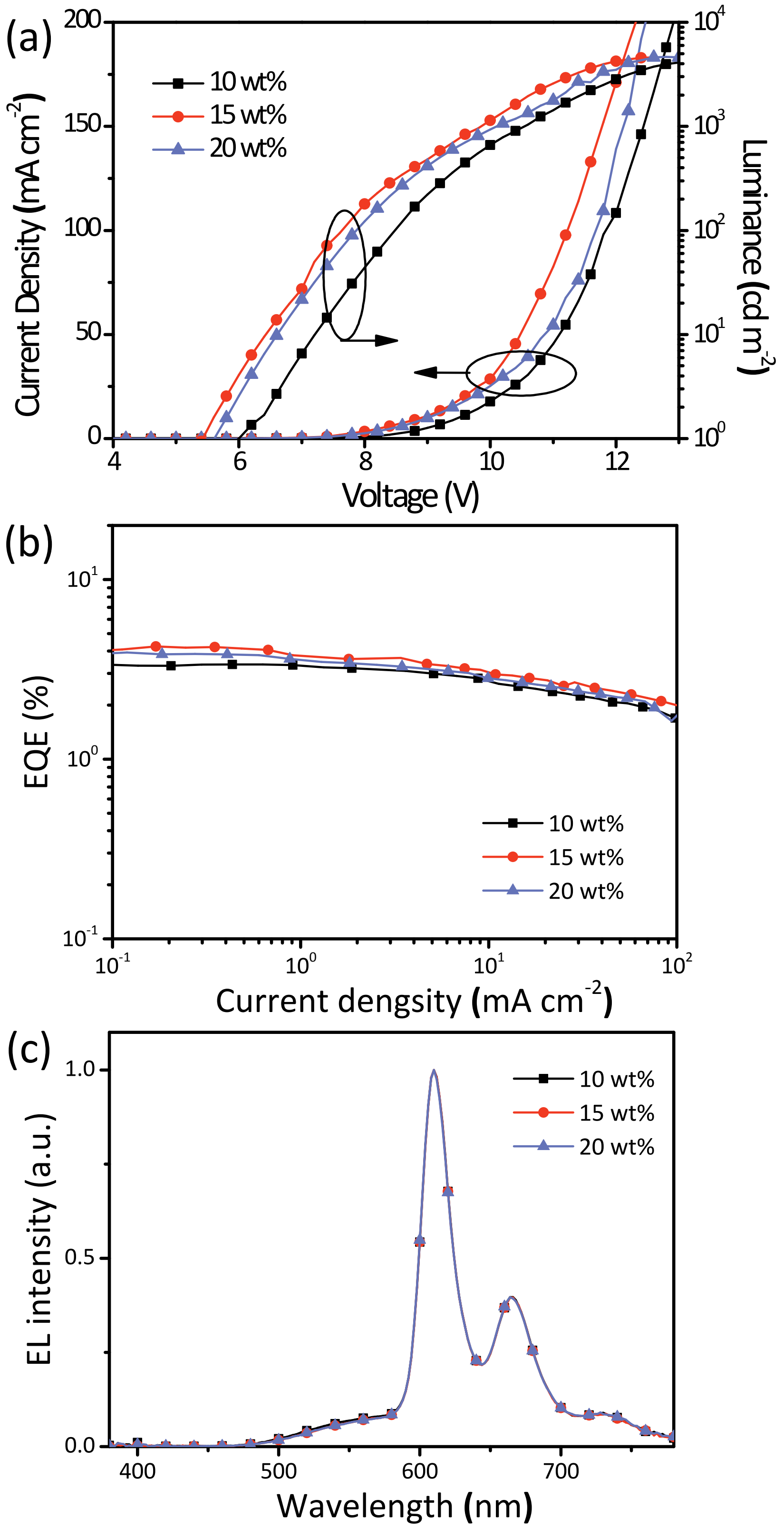

Figure S6. (a) Luminance-current density-voltage, (b) EQE-current density and (c) normalized EL spectra of the TAF-OLEDs based on DC-ACR as an assistant dopant at various doping concentrations in a structure of ITO/PEDOT:PSS (40 nm)/2 wt% DBP:x wt% DC-ACR:CBP (40 nm)/TmPyPB (55 nm)/LiF (1 nm)/Al (100 nm).

5. Exciton dynamics in DC-ACR based TAF-OLED

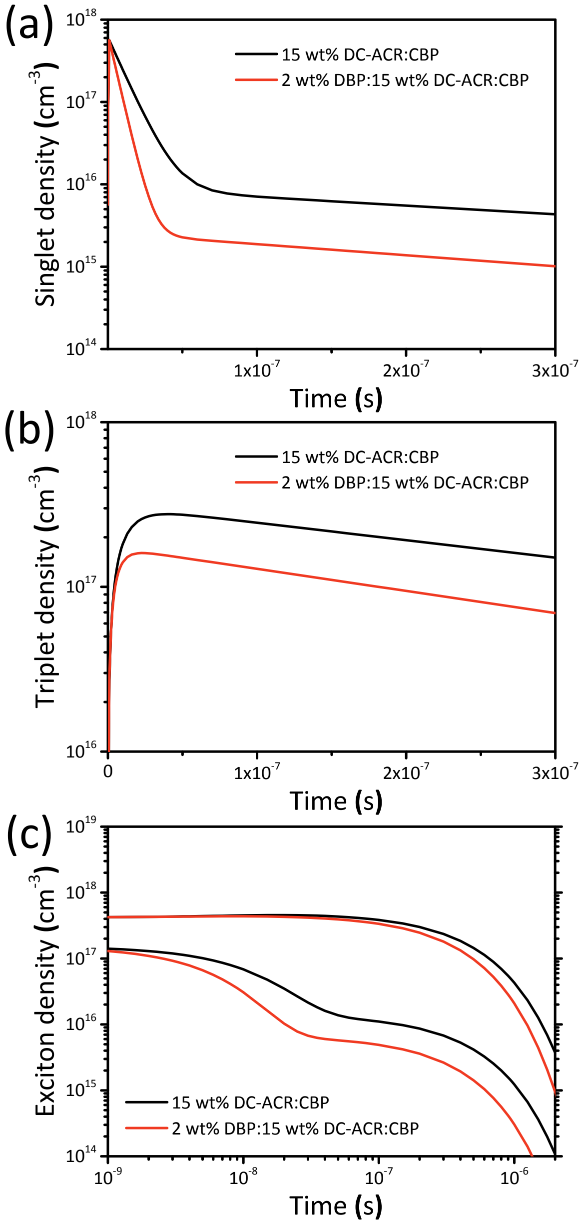

Figure S7. Dependence of calculated singlet density (a) and triplet density (b) in a 15 wt% DC-ACR:CBP co-coped film as a function of time with ($k_{ET} = 8.8 \times 10^7\ s^{-1}$, red lines) or without ($k_{ET} = 0\ s^{-1}$, black lines) Förster energy transfer. The exciton density is calculated using Equation (5) and (6) with $k_r^S = 3.7 \times 10^6\ s^{-1}$, $k_{ISC} = 4.6 \times 10^7\ s^{-1}$, $k_{RISC} = 2.6 \times 10^5\ s^{-1}$, $k_{nr}^S = 4.3 \times 10^7\ s^{-1}$ and $k_{nr}^T = 1.2 \times 10^6\ s^{-1}$. (c) The calculated singlet and triplet exciton densities in a 15 wt% DC-ACR:CBP co-coped film under electrical excitation as a function of time with or without Förster energy transfer using Equation (8) and (9).

Reference

1. X. Cai, X. Li, G. Xie, Z. He, K. Gao, K. Liu, D. Chen, Y. Cao and S.-J. Su, *Chem. Sci.*, 2016, **7**, 4264-4275.
2. Y. Tao, K. Yuan, T. Chen, P. Xu, H. Li, R. Chen, C. Zheng, L. Zhang and W. Huang, *Adv. Mater.*, 2014, **26**, 7931-7958.
3. Q. Zhang, H. Kuwabara, W. J. Potscavage, Jr., S. Huang, Y. Hatae, T. Shibata and C. Adachi, *J. Am. Chem. Soc.*, 2014, **136**, 18070-18081.
4. H. Uoyama, K. Goushi, K. Shizu, H. Nomura and C. Adachi, *Nature*, 2012, **492**, 234-238.
5. K. Goushi, K. Yoshida, K. Sato and C. Adachi, *Nat. Phot.*, 2012, **6**, 253-258.
6. H. Tanaka, K. Shizu, J. Lee and C. Adachi, *J. Phys. Chem. C*, 2015, **119**, 2948-2955.
7. C. Li, L. Duan, D. Zhang and Y. Qiu, *ACS Appl. Mater. Interfaces*, 2015, **7**, 15154-15159.